Showcasing research on G-quadruplex based aptasensing approaches for the detection of human angiotensinogen protein from Professor Yang Zhang's laboratory, College of Science, Harbin Institute of Technology (Shenzhen), Shenzhen, China.

Fluorescence detection of the human angiotensinogen protein by the G-quadruplex aptamer

As an important part of the renin–angiotensin system (RAS), angiotensinogen (AGT) is a precursor of angiotensin, which can be potentially used as a biomarker of diseases with RAS alterations. AGT is closely related to angiogenesis-dependent diseases, such as cancers, cardiovascular diseases, and hypertension.

In this work, two simple but effective biosensing approaches based on the G-quadruplex aptamer were developed for the fluorescence detection of human AGT protein.

As featured in:

See Yang Zhang *et al.*, *Analyst*, 2022, **147**, 4040.

ROYAL SOCIETY OF CHEMISTRY

rsc.li/analyst

Registered charity number: 207890

Analyst

ROYAL SOCIETY OF CHEMISTRY

PAPER

View Article Online
View Journal | View Issue

Cite this: *Analyst*, 2022, **147**, 4040

Fluorescence detection of the human angiotensinogen protein by the G-quadruplex aptamer†

Hui Xi,[a] Hanlin Jiang,[a] Mario Juhas[b] and Yang Zhang *[a]

Received 30th June 2022,
Accepted 2nd August 2022

DOI: 10.1039/d2an01057g

rsc.li/analyst

Noncanonical G-quadruplex nucleic acid structures can be used as probes in biosensors for the detection of metal ions, proteins and nucleic acids. Angiotensinogen (AGT) is a glycosylated globulin found in serum, which can regulate blood pressure and body fluid homeostasis. AGT is an important part of the renin–angiotensin system (RAS) and can be potentially used as a biomarker of diseases with RAS alterations. G-quadruplex based biosensors can detect targets with high accuracy and speed and low cost. Employing the magnetic bead enrichment method we constructed a reliable and efficient fluorescent biosensor platform for G-quadruplex based detection of the human AGT protein. The primary antibody in our biosensor is recognized by fluorescently labeled secondary antibodies, which leads to the detection of AGT captured by the G-quadruplex aptamer coupled magnetic beads. This G-quadruplex based fluorescent biosensor designed with a detection limit of 5×10^{-5} mg mL^{-1} was used for the successful detection of AGT at the cellular level. Our G-quadruplex based fluorescent biosensor will contribute to the more reliable and efficient detection of AGT.

1. Introduction

Angiotensin is a vasoconstrictive peptide, which regulates the secretion of aldosterone. It is an important part of the renin–angiotensin system (RAS).[1] Angiotensinogen (AGT) catalyzed by the renin enzyme forms angiotensin I (Ang I), which in turn is coverted to angiotensin II (Ang II) by the angiotensin converting enzyme (ACE). AGT and Ang II regulate blood pressure and corresponding physiological responses.[2] AGT and Ang II are also closely related to angiogenesis, alterations in which cause a variety of pathological states, including ischemic heart disease,[3] peripheral arterial occlusive disease,[4] cancer,[5] and nervous system disease.[6] Genetic mutations in AGT also lead to susceptibility to essential hypertension, and renal tubular dysgenesis, respectively.[7,8]

The rapid spread of SARS-CoV-2 represents a threat to public health. Sequencing and structure analysis of SARS-CoV-2 led to a better understanding of its interaction with angiotensin converting enzyme 2 (ACE 2), which is closely related to angiotensin.[9,10] As there are only a few methods available for the detection of angiotensin and AGT, novel biosensors can contribute greatly to reliable and efficient AGT detection.

Molecular biology advances, such as the Human Genome Project revealed that DNA and RNA do not only store and transmit genetic information, but also interact with other substances by changing their own spatial structures.[11,12] Nucleic acid aptamer is an ideal molecular recognition element for biosensors[13] with a number of advantages, such as easy modification and synthesis *in vitro*, and low price.

G-quadruplex is a noncanonical spatial structure of nucleic acids rich in guanine.[14–16] G-quadruplex has many characteristics suitable for biosensors. These include thermodynamic and chemical stability, non-immunogenicity, high target interaction specificity, ease of manufacture and storage, and unique folding properties leading to different conformations.[17,18] It can be used as an unlabeled signal probe molecule for the detection of metal ions, organic macromolecules, nucleic acids, peptides, *etc*.[12,19–21]

The advantages of the G-quadruplex based biosensor include high accuracy, speed and low cost of detection and quantitative analysis of substances.[22] We have previously reported Cell-SELEX-based identification of a G-quadruplex forming DNA aptamer (C20-4 min).[23,24] C20-4 min was screened from the SELEX Library, 5′-ATCCAGAGTGACG-CAGCA-40N-TGGACACGGTGGCTTAGT-3′ (*N* represents a random sequence). C20-4 sequence 5′-GGGTGGGGGGGTGG-3′

[a]*College of Science, Harbin Institute of Technology (Shenzhen), Shenzhen, Guangdong, 518055, China. E-mail: zhangyang07@hit.edu.cn*
[b]*Medical and Molecular Microbiology Unit, Department of Medicine, Faculty of Science and Medicine, University of Fribourg, Fribourg, 1700, Switzerland*
† Electronic supplementary information (ESI) available. See DOI: https://doi.org/10.1039/d2an01057g

conforms to the general sequence formula of the G-quadruplex structure: $G_{(\geq 2)}N_xG_{(\geq 2)}N_yG_{(\geq 2)}N_zG_{(\geq 2)}$ (N is the nucleotide, and x, y and z can be different numbers).[24] Bioinformatics analysis of the transcriptome showed interactions between G-quadruplex aptamer C20-4 min and AGT. G-quadruplex was shown to upregulate the gene expression of AGT,[24] thus suggesting that C20-4 min may regulate the function of AGT. Therefore, we set out to explore the potential of the G-quadruplex forming aptamer C20-4 min as a biorecognition element in the biosensor for AGT detection.

Biosensors convert bioactive expression signals into easy to observe electrical[25] and optical signals.[26] The fluorescence signal reading method is universal, sensitive, efficient and simple without sample fixation.[27] The fluorescence signal change is reflected in the quenching or the enhancement of the fluorescence signal, as well as in the shift of spectral characteristic wavelength.[28] Fluorescence signal change is measured after binding to the target substance, thus allowing engineering of a fluorescence sensing platform.[29]

In this work, we set out to develop a G-quadruplex based fluorescent biosensor for the detection of AGT. First, we identified the G-quadruplex aptamer which interacts strongly with AGT and used fluorescence specific lighting to verify that the screened aptamer was indeed a G-quadruplex structure. Then, we employed the principle of biotin–streptavidin interaction for enrichment,[30] and used biotin modified aptamers as probes to capture AGT. Using the antigen–antibody interaction,[31] we constructed the system composed of "Dynabeads/G-quadruplex/AGT/primary antibody/fluorescence labeled secondary antibody". We showed that the fluorescently labeled secondary antibody can detect the primary antibody by visible fluorescent signal and indirectly detect the target substance. Our G-quadruplex-based system can be used for the fluorescence detection of human AGT.

2. Experimental section

2.1. Reagents and materials

Phosphate buffered saline (PBS), Dynabeads™ M-270 streptavidin, Dynabeads™ protein G, angiotensinogen recombinant rabbit monoclonal antibody (primary antibody), goat anti-rabbit IgG (H + L) highly cross-adsorbed secondary antibody, Alexa Fluor Plus 488 (secondary antibody), Pierce® IP lysis buffer Pierce™ IP were used. The concentrations of Dynabeads™ M-270 streptavidin (stored at 4 °C) and Dynabeads™ protein G (stored at 4 °C) were 10 mg mL^{-1} and 30 mg mL^{-1}, respectively. The concentrations of the primary antibody (stored at −20 °C) and secondary antibody (stored at 4 °C) were 1 mg mL^{-1} and 2 mg mL^{-1}, respectively. 1 × TE buffer was purchased from Sangon Biotech. *N*-Methylporphyrin dipropionic acid IX (NMM) was purchased from J&K Scientific. 2 mM NMM stock solution was stored at −20 °C. Bovine serum albumin (BSA) was purchased from BioFroxx. Recombinant human angiotensinogen protein (AGT) was purchased from Abcam. AGT is a full-length protein expressed by HEK 293 cells with a molecular weight of 51 kDa. AGT was resuspended in 200 μL of deionized water to prepare 0.5 mg mL^{-1} stock solution (stored at −80 °C). HUVEC, complete media with 0.25% trypsin–EDTA was used. Aptamers were purchased from Thermo Fisher Scientific and purified by HPLC. The stock solutions of aptamers (100 μM) were dissolved in TE buffer and stored at −20 °C. Aptamers and their sequences are shown in Table 1.

2.2. NMM specific lighting G-quadruplex

Specific binding of NMM with parallel G-quadruplex (but not with trimer, dimer and single chain) produces strong fluorescence. The fluorescence spectrometer parameters were set as follows: excitation 399 nm, emission 610 nm and slit length 10 nm.[32] NMM stock solution was diluted to optimize the concentration of fluorescent reporter molecules. NMM and different concentrations (0.001–0.5 μM) of C20-4 min and its mutant nucleic acid were dissolved in PBS for fluorescence detection.

2.3. Microscale thermophoresis (MST) to characterize the potential binding ability of G-quadruplex and AGT

MST is used to analyze the interaction between biomolecules (proteins, RNA, DNA, small molecules and ions).[33] AGT was expressed and purified as a binding target. A series of concentration titration of the AGT protein were prepared by quantifying the dissociation constant of nucleic acid aptamer. The intermolecular binding affinity K_d was automatically calculated from the NanoTemper binding curve in MST.[34] Proteins without fluorescence signals were detected by DNA aptamers labeled with fluorescein isothiocyanate (FITC). The interaction between G-quadruplex and AGT was measured by MST. MST assays were carried out on an instrument (NanoTemper) using the 'nano-blue' channel. AGT with gradient concentrations (0.00762939–250 nM) was mixed with C20-4 min-FITC and NC-FITC (4 nM) in PBS. The samples were incubated at room temperature in the dark for 30 min, and analyzed by MST. The data were fitted by NanoTemper for the analysis of K_d.

Table 1 Aptamers used in this study

Aptamer	Sequence (5′ → 3′)
C20-4 min	5′-GGGTGGGGGGGTGG-3′
C20-1&3 min	5′-GGGTGGGTGGGTGG-3′
2T mutation	5′-GGGTGTGGGTGTGG-3′
3T mutation	5′-GGGTGTGTGTGTGG-3′
GT mutation	5′-GTGTGTGTGTGTGT-3′
C20-4 min-FITC	5′-FITC-GGGTGGGGGGGTGG-3′
NC-FITC	5′-FITC-ATGCATGCATGCAT-3′
C20-4 min-biotin	5′-Biotin-GGGTGGGGGGGTGG-3′
C20-1&3 min-biotin	5′-Biotin-GGGTGGGTGGGTGG-3′
2T mutation-biotin	5′-Biotin-GGGTGTGGGTGTGG-3′
3T mutation-biotin	5′-Biotin-GGGTGTGTGTGTGG-3′
GT mutation-biotin	5′-Biotin-GTGTGTGTGTGTGT-3′
NC-biotin	5′-Biotin-ATGCATGCATGCAT-3′
Biotin-C20-4 min-FITC	5′-Biotin-ATGCATGCATGCAT-FITC-3′

2.4. Construction of the G-quadruplex based detection system employing magnetic bead enrichment

The nucleic acid concentration was optimized and enriched by Dynabeads. The Dynabeads bottle was first mixed by vortex and 10 μL Dynabeads–streptavidin were taken for the subsequent steps. Following magnetic frame adsorption, the supernatant was removed, and washed twice with PBS. Next, gradient concentrations (10^{-8}–1 μM) of Biotin-C20-4 min-FITC were added. Samples without DNA aptamer were used as a blank control. The mixture was incubated on a vertical mixer for 1 h. Following magnetic frame adsorption, the supernatant was removed, washed 3 times with PBS, and the unbound nucleic acid was removed. The microplate reader parameters for the detection of the fluorescence of Dynabeads were set as follows: excitation wavelength of 485/20 nm and emission wavelength of 528/20 nm.

AGT was detected based on magnetic bead enrichment. According to the above steps, the "Dynabeads/aptamer" system was constructed. Gradient concentrations of AGT (0.00005–0.001 mg mL^{-1}) were added. Samples without AGT were used as the blank control. The mixture was incubated for 1 h and the above steps were repeated to wash and remove the unbound protein. The primary antibody (0.001 mg mL^{-1}, 1 : 1000 dilution) was added and incubated for 1 h. The above steps were repeated to remove the redundant primary antibody. Secondary antibody (0.002 mg mL^{-1}, 1 : 1000 dilution) was added and incubated for 1 h. The above steps were repeated to remove excess fluorescence of the secondary antibody. A microplate reader was used to detect the fluorescence of Dynabeads and to analyze the affinity of G-quadruplex to AGT. In the negative control, AGT was replaced with BSA.

2.5. AGT detection at the cellular level using the G-quadruplex based fluorescent biosensor

The native form of the AGT protein was extracted from human umbilical vein endothelial cells (HUVEC).[35] HUVEC were grown in the culture medium (90%DMEM + 10%FBS). The cells were then lysed using lysis buffer (25 mM Tris·HCl pH 7.4, 150 mM NaCl, 1% NP-40, 1 mM EDTA, 5% glycerol, 1 × Halt™ Phosphatase Inhibitor Single-Use Cocktail) and incubated on ice for 5 min. The lysate was transferred to a microcentrifuge tube and centrifuged at 13 000*g* and 4 °C for 10 min. The supernatant was transferred to a new test tube for protein concentration determination. The total protein concentration of HUVEC cell extraction is approximately 1100 μg mL^{-1}, which is determined by the bicinchoninic acid (BCA) assay. The magnetic beads were incubated with angiotensinogen antibody (IgG antibody) for 30 min, and the magnetic beads were washed to remove unbound antibodies. The cell lysate was added and incubated for 30 min, and the magnetic beads were washed to remove the unbound protein. C20-4 min-FITC was then incubated with the bead system for 30 min, and then washed to remove the unbound probe. NC-FITC was used as the negative control. The fluorescence signal was detected using a microplate reader.

3. Results and discussion

3.1. Interaction between the G-quadruplex aptamer and AGT

MST was performed to investigate the interaction between the G-quadruplex (C20-4 min) aptamer and the AGT protein and to analyze potential binding events. The aptamer NC was used as the negative control. Dissociation constants of the AGT protein were quantified with C20-4 min and NC. A titration series of AGT (0.00762939–250 nM) with constant concentrations of C20-4 min-FITC and NC-FITC (4 nM) was prepared. At different AGT concentrations, the fluorescence signal of the DNA aptamer after standardized treatment forms a binding curve for K_d fitting.[36] The smaller the equilibrium dissociation constant (K_d), the greater the affinity between molecules, and the less likely it is to dissociate.[37] K_d is calculated automatically according to the binding, and the curve is fitted by NanoTemper analysis in MST. The fitting formula of the K_d model is as follows:

$$f(c) = \text{unbound} + (\text{bound} - \text{unbound}) \times \frac{c + c_{\text{target}} + K_d - \sqrt{(c + c_{\text{target}} + K_d)^2 - 4cc_{\text{target}}}}{2c_{\text{target}}} \quad (1)$$

C20-4 min/AGT and NC/AGT values are 2.3865 ± 1.7198 × 10^{-9} M (Fig. 1A) and 1.1710 ± 0.8896 × 10^{-7} M (Fig. 1B). The $K_{d(\text{C20-4 min})}$ is significantly lower than $K_{d(\text{NC})}$, indicating that the C20-4 min G-quadruplex aptamer can bind to AGT with high affinity, but not NC. This analysis shows that the C20-4 min aptamer can be used as a signal recognition element for the detection of AGT. Three groups of experiments performed in parallel confirmed that $K_{d(\text{C20-4 min})} < K_{d(\text{NC})}$ (Fig. 1C).

3.2. Construction of the *N*-methylporphyrin dicarboxylic acid IX (NMM)/G-quadruplex "signal on" fluorescent probe

NMM is a water-soluble asymmetric porphyrin with excellent optical properties. NMM shows high fluorescence and energy levels in organic solvents. The fluorescence of NMM in aqueous solution is very low. Water can quench the fluorescence of NMM by reducing the energy level of NMM, thus allowing an easy non radiative transition. A red shift occurs at higher concentrations.[32] The NMM/G-quadruplex illuminated fluorescent probe can be designed to confirm the G-quadruplex structure of the selected aptamers. The fluorescence excitation wavelength is 399 nm and the strongest emission peak wavelength is 610 nm.[32,38] This system has excellent selectivity for G-quadruplex, while aptamers with other structures do not have this property. Based on this specificity, NMM/G-quadruplex "signal on" fluorescent probes can be designed. NMM itself has weak fluorescence, and excessive concentration will produce a large background signal, therefore the NMM dosage needs to be optimized. The optimum reaction concentration of NMM was determined to be 0.6 μM using an enzyme labeling instrument and a fluorescence spectrometer (ESI and Fig. S1†).

Fig. 2A shows the principle of the specific lighting effect of NMM on G-quadruplex. The sequence of C20-4 min conforms

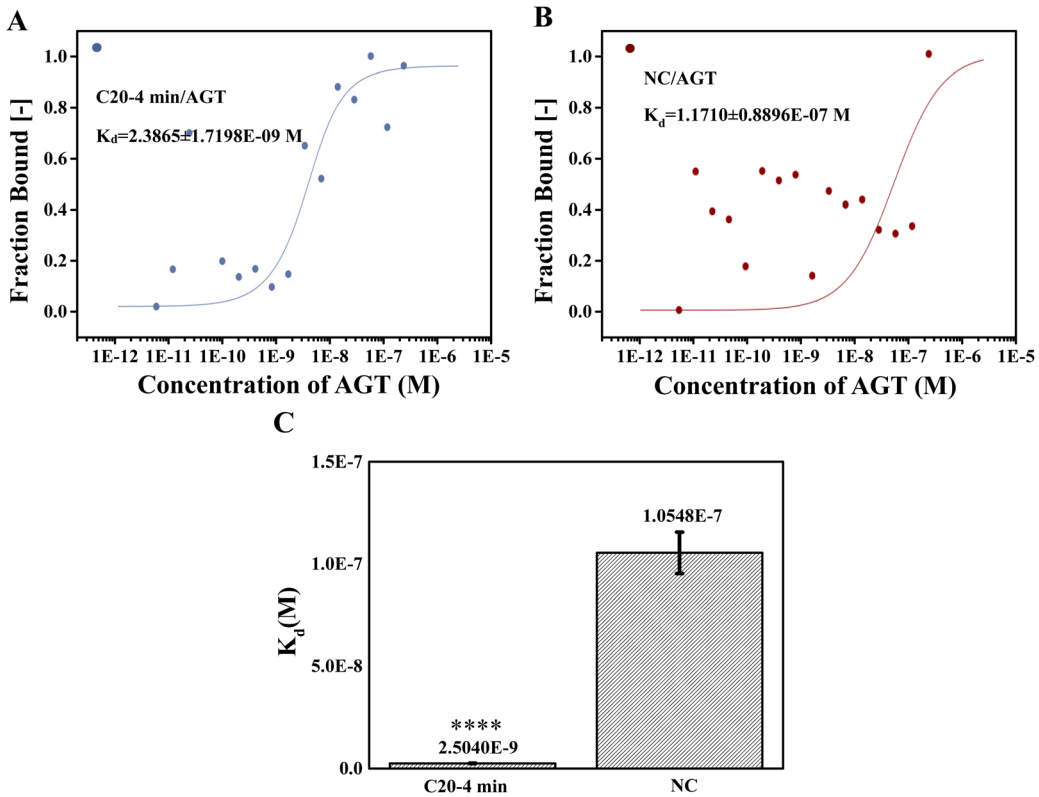

Fig. 1 Interaction between AGT and C20-4 min or NC aptamers. (A) MST analysis of the dose–response curve of the binding between AGT and C20-4 min aptamer. (B) MST analysis of the dose–response curve of the binding between AGT and NC aptamer. (C) Interaction between nucleic acid aptamers and AGT (average $K_{d(C20\text{-}4\ min)}$ = 2.5043 ± 0.1089 × 10^{-9}; average $K_{d(NC)}$ = 1.0548 ± 0.1018 × 10^{-7}; n = 3). Numbers represent mean and standard errors from three independent replicates (****P < 0.0001).

to the general formula of single molecule G-quadruplex, $G_{(\geq 2)}N_xG_{(\geq 2)}N_yG_{(\geq 2)}N_zG_{(\geq 2)}$, thus suggesting that C20-4 min forms a G-quadruplex structure. Combining NMM and C20-4 min (0.01–0.5 μM) in PBS led to the enhancement of the fluorescence signal. The curve of the change of signal intensity with the concentration of G-quadruplex shows that the fluorescence intensity increases with the increase of concentration (ESI and Fig. S1E†). NMM/C20-4 min is a "signal on" fluorescent probe, thus proving that C20-4 min has a parallel G-quadruplex conformation. C20-4 min related nucleic acids with point mutations include C20-1&3 min; 2T mutation; 3T mutation and GT mutation. Modifications of their concentration have an effect on the fluorescence of the NMM system ($\Delta F = F_{NMM/Aptamer} - F_{NMM}$, $F_{NMM/Aptamer}$ is the fluorescence of NMM after binding to the aptamer; F_{NMM} is the background fluorescence value of NMM) (n = 3, RSD ≤ 5%) (Fig. 2B). The system's fluorescence increases with increasing DNA concentration. Notably, each mutation has different effects on NMM. The level of fluorescence enhancement is as follows: C20-4 min ≈ C20-1&3 min > 2T mutation > 3T mutation > GT mutation. This indicates that the greater the degree of mutation, the stronger disruption effect on the structure of parallel G-quadruplex. Metal ions affect the formation of the G-quadruplex structure. K^+ promotes the formation of a parallel G-quadruplex, while Li^+ is not conducive to the formation of G-quadruplex (Fig. 2C).

We construct the NMM/C20-4 min label-free "signal on" fluorescent probe to study its detection on AGT. When NMM and C20-4 min are combined with AGT (0.001–0.00005 mg mL^{-1}) in PBS, the fluorescence intensity remains unchanged, and the detection is unsuccessful (Fig. 2D). The fluorescence intensity does not change with the changes of AGT concentrations. This can be caused by NMM occupying the binding site of the G-quadruplex. Consequently, the protein cannot bind or the protein binds to other sides of the G-quadruplex. AGT has no effect on the whole fluorescence system, therefore AGT cannot be detected directly by the NMM/G-quadruplex probe.

3.3. Detection of AGT by magnetic bead enrichment based on the G-quadruplex aptamer

Because the NMM/G-quadruplex fluorescent probe system cannot detect AGT directly as shown above, we used instead the magnetic bead enrichment method. The detection principle of the magnetic bead enrichment method is shown in Fig. 3A. Due to the biotin–streptavidin interaction, Dynabeads–streptavidin captures biotin-labeled aptamers. MST experiment shows that the G-quadruplex aptamer can bind to AGT thus

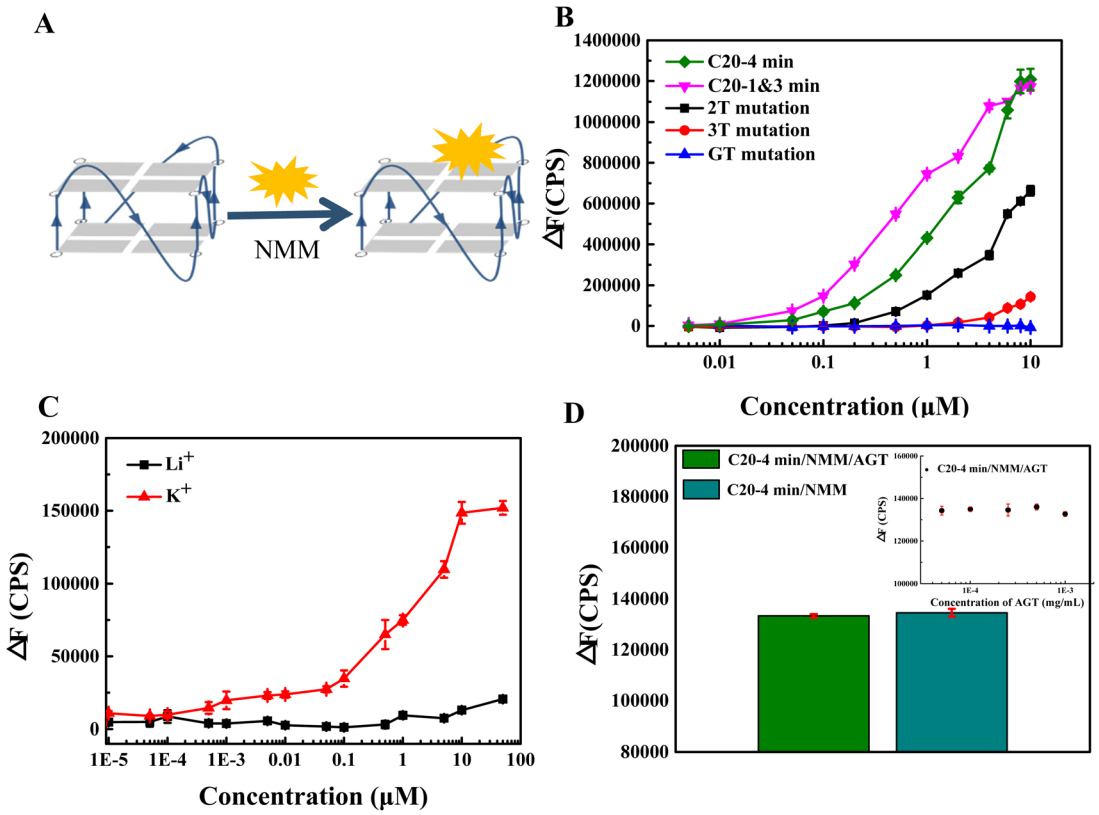

Fig. 2 (A) The mechanism of NMM "light on" G-quadruplex. (B) Analysis of the fluorescence intensity of different nucleic acids lighted by NMM. (C) The effect of metal ions on G-quadruplex (C20-4 min). Fluorescence intensity of the NMM/C20-4 min fluorescence system in different monovalent cation buffer solutions. (D) Detection of AGT using the NMM/G-quadruplex fluorescent probe. Bar chart shows the fix concentration of AGT detected by NMM/C20-4 min (n = 3, RSD ≤ 5%). The line chart shows the relationship between the fluorescence intensity of NMM/C20-4 min and concentrations of AGT.

allowing the formation of the "Dynabeads/G-quadruplex/AGT" system. The G-quadruplex coupled beads bound AGT can be recognized by AGT monoclonal antibody. Combined with fluorescently labeled secondary antibodies, AGT was detected and quantified indirectly.

The binding ability between magnetic beads and biotin modified nucleic acid, and the concentration of biotin labeled nucleic acid adsorbed by magnetic beads was analyzed. Magnetic beads (10 μL) and biotin-C20-4 min-FITC (10^{-8}–1 μM) were incubated for 1 h. Magnetic beads reached saturation at an aptamer concentration of 10 nM. Therefore, we chose the amount of magnetic beads to be 10 μL in subsequent experiments, and the optimal concentration of nucleic acid aptamer was 10 nM. (Fig. 3B).

The specificity of the interaction between nucleic acid and AGT was analyzed. MST experiments show that AGT can be specifically recognized by C20-4 min. The increased mutation level leads to the destruction of the structure of the G-quadruplex and potential reduction of its target binding ability. Different aptamers were selected as capture probes on enriched magnetic beads, namely C20-4 min-Biotin, C20-1&3 min-Biotin, 2T mutation-Biotin, 3T mutation-Biotin, GT mutation-Biotin, and NC-Biotin. Samples without the aptamer were used as the blank control. The detection system was constructed to capture AGT. The concentration of AGT used was 0.001 mg mL^{-1}. AGT was shown to bind with C20-4 min with high specificity, thus generating strong fluorescence signals. The fluorescence intensity decreased with the increased mutation degree (Fig. 3C). The destruction of the G-quadruplex and reduction of its binding ability with AGT suggest that G-quadruplex aptamers capture AGT due to their spatial structures.

Detection limit of the magnetic bead enrichment method for detecting AGT based on G-quadruplex C20-4 min was analyzed. A series of AGT concentrations, 0.001 mg mL^{-1}, 0.0005 mg mL^{-1}, 0.00025 mg mL^{-1}, 0.0001 mg mL^{-1}, and 0.00005 mg mL^{-1}, were used. The samples without AGT were used as the blank control. Increasing the AGT concentration led to an increase of the AGT protein bound to the magnetic beads and higher fluorescence intensity (Fig. 3D). The relationship between the relative fluorescence intensity and AGT concentration is $F = 2.538E7C_{AGT} + 14\,586$ ($R^2 = 0.96624$). When the signal-to-noise ratio is 3 (S/N = 3), the detection limit LOD is 5×10^{-5} mg mL^{-1} (9.8×10^{-10} M). The molecular weight of AGT is 51 kDa. There are very few methods available for detecting AGT, and the biosensor-based detection of AGT has never

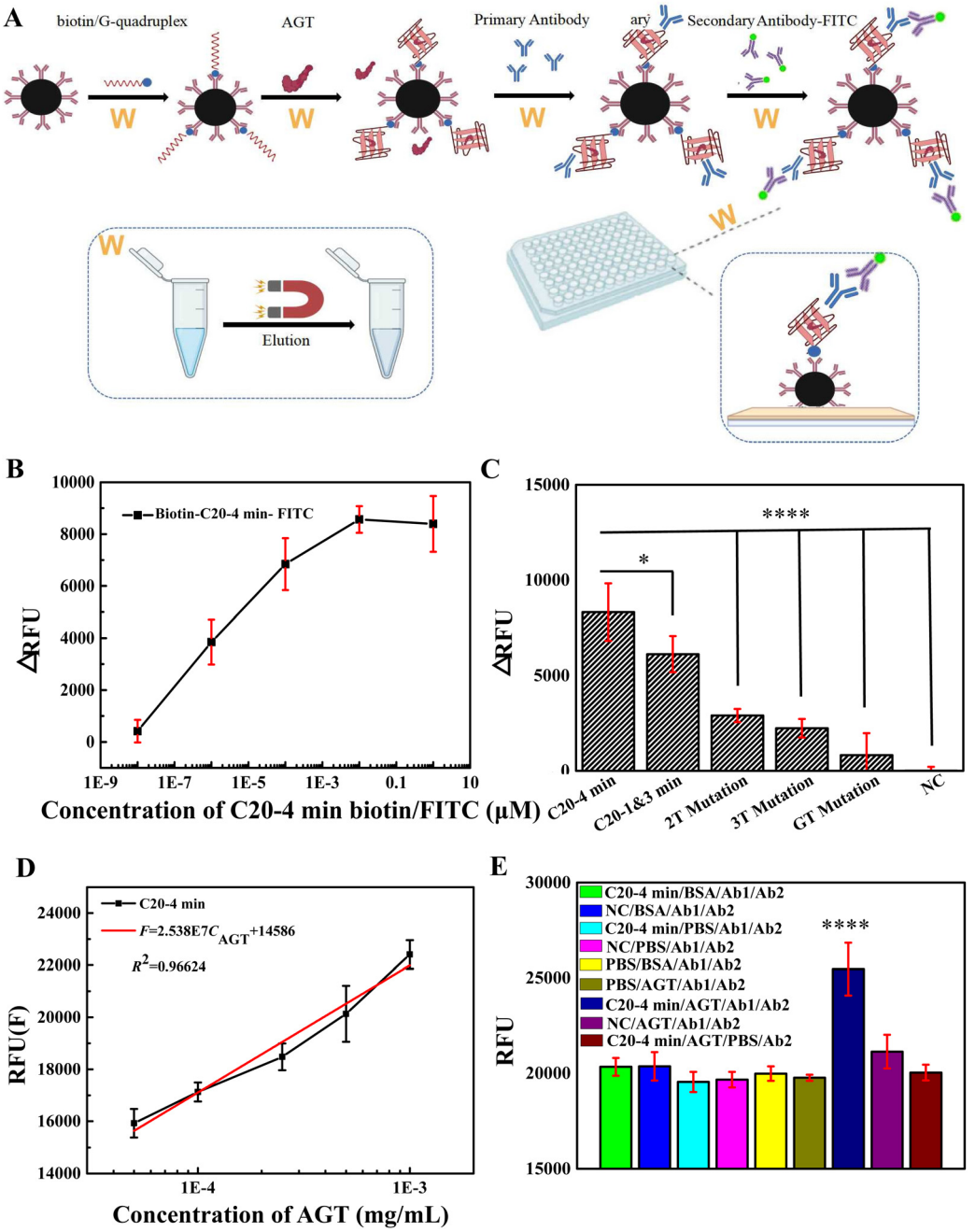

Fig. 3 (A) Schematic diagram of the magnetic bead enrichment method. (1) Streptavidin modified magnetic beads were used to capture biotin labeled aptamers; (2) target protein AGT was added, and G-quadruplex aptamer captured AGT onto the magnetic beads; (3) AGT monoclonal antibody was added to the system to bind with AGT; and (4) fluorescent secondary antibody was added to detect AGT. In each step, free substances in the solution were removed by washing with PBS. (B) Determination of the optimal concentration of biotin labeled aptamers adsorbed by magnetic beads. Analyzed concentrations of biotin-C20-4 min-FITC: 1 μM, 10^{-2} μM, 10^{-4} μM, 10^{-6} μM, 10^{-8} μM, 0 μM. (C) Detection of AGT by different aptamers (C20-4 min-biotin, C20-1&3 min-biotin, 2T mutation-biotin, 3T mutation-biotin, GT mutation-biotin, and NC-biotin; *P < 0.05, ****P < 0.0001). (D) The linear relationship of the target protein based on the G-quadruplex. $LOD_{(AGT)}$ = 5 × 10^{-5} mg mL^{-1} (9.8 × 10^{-10} M) (S/N = 3). (E) Specificity of the G-quadruplex based AGT biosensor (Ab1: primary antibody; Ab2: secondary antibody; ****P < 0.0001).

been reported. Suzaki *et al.* developed an enzyme linked immunosorbent assay (ELISA) for AGT detection.[39] Compared to traditional ELISA, our method has a number of advantages. Besides providing a new detection platform for detecting AGT, the operation of our method is very simple and straightforward. In addition, aptamers have many advantages, such as easy *in vitro* synthesis, small size, low price, and easy modification.

Next, we explored the specificity of the magnetic bead enrichment method for detecting AGT based on G-quadruplex

and investigated whether antibodies and other proteins could be affected by the modification of the composition of the magnetic bead system. The protein concentration was set as 0.001 mg mL^{-1}. Different systems were tested, including "C20-4 min/BSA/primary antibody/secondary antibody", "NC/BSA/primary antibody/secondary antibody", "C20-4 min/PBS/primary antibody/secondary antibody", "NC/PBS/primary antibody/secondary antibody", "PBS/BSA/primary antibody/secondary antibody", "PBS/AGT/primary antibody/secondary antibody", "C20-4 min/AGT/primary antibody/secondary antibody", "NC/AGT/primary antibody/secondary antibody", "C20-4 min/AGT/PBS/secondary antibody". As shown in Fig. 3E, only "C20-4 min/AGT/primary antibody/secondary antibody" emitted clear fluorescence signals, thus indicating that C20-4 min can specifically capture and detect AGT. Control protein (BSA), "C20-4 min/BSA/primary antibody/secondary antibody" and "NC/BSA/primary antibody/secondary antibody" emitted only background signals, thus confirming the high specificity of this method. "C20-4 min/PBS/primary antibody/secondary antibody" and "NC/PBS/primary antibody/secondary antibody" showed that nucleic acid could not bind directly to the primary antibody and secondary antibody. The G-quadruplex nucleic acid could capture only AGT, and the antibody used in the system had no effect on the experimental result. "PBS/BSA/primary antibody/secondary antibody" and "PBS/AGT/primary antibody/secondary antibody" showed that magnetic beads could not bind directly with proteins and capture proteins by enriching aptamers. "NC/AGT/primary antibody/secondary antibody" indicates that G-quadruplex C20-4 min has high affinity to AGT. "C20-4 min/AGT/PBS/secondary antibody" shows that the secondary antibody cannot directly bind to AGT. The fluorescent secondary antibody can only bind with the primary antibody through the antigen–antibody interaction to detect AGT indirectly.

The magnetic bead enrichment method can be used to detect AGT based on G-quadruplex. The system can detect AGT both qualitatively and quantitatively with good specificity and high accuracy. This biosensor technology has therefore significant potential in the diagnosis of diseases using the AGT as a biomarker.

We successfully engineered a system for the fluorescence detection of human AGT based on the G-quadruplex aptamer. In order to improve the system's sensitivity, the G-quadruplex aptamers with stronger affinity to AGT can be screened or

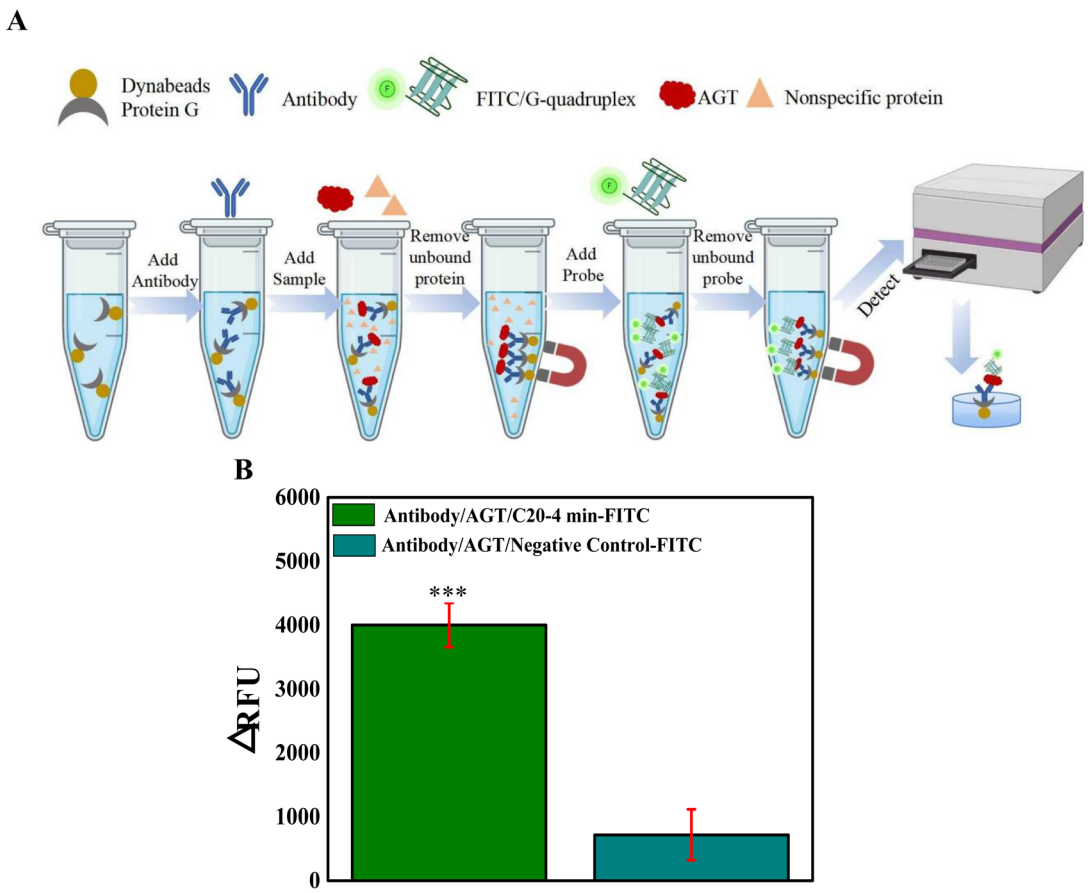

Fig. 4 (A) Schematic diagram of detection of the native form of AGT protein by immunoprecipitation and the FITC labeled G-quadruplex aptamer. (B) G-quadruplex aptamer can detect AGT in cells, while the negative control (NC) cannot. Error bars represent mean and standard errors from three independent replicates (***$P < 0.005$).

modified. In the future, the system can be further optimized to shorten the detection time and to use other signal conversion methods.

3.4. Detection of the native form of AGT in cells by the G-quadruplex based fluorescent biosensor

Immunoprecipitation can separate and concentrate specific proteins from thousands of different proteins.[40] The principle of protein detection by immunoprecipitation based on G-quadruplex is shown in Fig. 4A. The Dynabeads-protein G binding IgG antibody is used to enrich the AGT protein, and fluorescence detection is achieved using the fluorescently labeled aptamer. HUVEC were cultured and lysed to extract the native form of the AGT protein from cells. The immunoprecipitated AGT protein from cells was used for interaction with the FITC labeled G-quadruplex aptamer. FITC labeled aptamer C20-4 min produced a fluorescent signal (Fig. 4B), thus showing that this G-quadruplex based fluorescent biosensor can be used for the qualitative detection of AGT in cells. The experiment conducted herein is a proof of the principle that our newly developed aptamer-based biosensor could not only detect recombinant protein but also the native form of the AGT protein. However, testing the biosensor response to different concentrations of native form of AGT and determining its limit of detection for native AGT are necessary and should be investigated in future studies.

4. Conclusion

Biosensors represent promising tools for reliable and efficient AGT detection. This work presents the successful fluorescence detection of human AGT based on a G-quadruplex aptamer. The G-quadruplex aptamers with high affinity for AGT were screened, and the binding ability of the selected G-quadruplex and its mutant sequences to AGT were characterized. A sensing platform employing the fluorescence signal output for detecting AGT based on G-quadruplex was constructed. NMM was used to construct a specific label free fluorescent biosensor and it was shown that it cannot detect AGT directly. A fluorescent biosensor platform utilizing antigen–antibody specific binding and magnetic bead enrichment based on the G-quadruplex aptamer was therefore designed for efficient and specific AGT detection. This novel biosensor exhibited strong fluorescence signals, which allowed successful AGT protein detection. Mutations led to the destruction of the G-quadruplex structure and reduction of the binding to AGT. The presented biosensor for AGT detection based on G-quadruplex aptamer C20-4 min achieved $LOD_{(AGT)} = 5 \times 10^{-5}$ mg mL^{-1}. Increased AGT concentration led to the increased quantity of the protein bound on the magnetic beads and higher fluorescence intensity. The G-quadruplex aptamer-based biosensor was also used for AGT detection at the cellular level. In the future, the conditions can be optimized to further improve the presented AGT detection biosensor platform. This novel biosensor system has important clinical applications and will contribute to the convenient and reliable detection of AGT protein in different diseases.

Author contributions

The manuscript was written through contributions of all authors.

Conflicts of interest

The authors declare no conflict of interest.

Acknowledgements

This work was supported by the Guangdong Basic and Applied Basic Research Foundation (2021A1515220115) and the Open Funding of the Key Laboratory of Zhejiang Province for Aptamers and Theranostic (2022ASC001).

References

1 R. Skrbic and R. Igic, *Peptides*, 2009, **30**, 1945–1950.
2 C. Ji, S. Yue, J. Gu, Y. Kong, H. Chen, C. Yu, Z. Sun and M. Zhao, *Sci. Total Environ.*, 2019, **697**, 134156.
3 S. C. Tyagi, *J. Cell. Biochem.*, 1997, **65**, 388–394.
4 P. Y. Lin, P. H. Sung, S. Y. Chung, S. L. Hsu, W. J. Chung, J. J. Sheu, S. K. Hsueh, K. H. Chen, R. W. Wu and H. K. Yip, *J. Clin. Med.*, 2018, **7**, 548.
5 H. K. Bid, R. D. Roberts, P. K. Manchanda and P. J. Houghton, *Mol. Cancer Ther.*, 2013, **12**, 1925–1934.
6 D. A. Greenberg and K. L. Jin, *Nature*, 2005, **438**, 954–959.
7 J. K. Fajar, B. S. Pikir, E. P. Sidarta, P. N. B. Saka, R. R. Akbar, F. Tamara, E. D. Mayasari, A. Gunawan and T. Heriansyah, *Gene Rep.*, 2019, **16**, 100421.
8 M.-H. Tseng, S.-M. Huang, M. Konrad, J.-L. Huang, S. W. Shaw, Y.-C. Tian, H.-Y. Chueh, W.-L. Fan, T.-W. Wu, J.-J. Ding, M.-C. Chiang and S.-H. Lin, *Cells*, 2021, **10**, 782.
9 J. Lan, J. Ge, J. Yu, S. Shan, H. Zhou, S. Fan, Q. Zhang, X. Shi, Q. Wang, L. Zhang and X. Wang, *Nature*, 2020, **581**, 215–220.
10 Q. Zhang, S. Lu, T. Li, L. Yu, Y. Zhang, H. Zeng, X. Qian, J. Bi and Y. Lin, *J. Exp. Clin. Cancer Res.*, 2019, **38**, 173.
11 W.-F. Yuan, L.-Y. Wan, H. Peng, Y.-M. Zhong, W.-L. Cai, Y.-Q. Zhang, W.-B. Ai and J.-F. Wu, *Cell Biochem. Funct.*, 2020, **38**, 524–532.
12 A. Ruscito, E. M. McConnell, A. Koudrina, R. Velu, C. Mattice, V. Hunt, M. McKeague and M. C. DeRosa, *Curr. Protoc. Chem. Biol.*, 2017, **9**, 233–268.
13 O. A. Alsager, S. Kumar and J. M. Hodgkiss, *Anal. Chem.*, 2017, **89**, 7416–7424.
14 Y. Zhang, B. S. Lai and M. Juhas, *Molecules*, 2019, **24**, 941.
15 Y. Sun, Y. Lin, R. Han, X. Wang and C. Luo, *Talanta*, 2019, **200**, 57–66.

16 R. Perrone, E. Butovskaya, S. Lago, A. Garzino-Demo, C. Pannecouque, G. Palu and S. N. Richter, *Int. J. Antimicrob. Agents*, 2016, **47**, 311–316.
17 F. Raguseo, S. Chowdhury, A. Minard and M. Di Antonio, *Chem. Commun.*, 2020, **56**, 1317–1324.
18 S. L. Noer, S. Preus, D. Gudnason, M. Aznauryan, J.-L. Mergny and V. Birkedal, *Nucleic Acids Res.*, 2016, **44**, 464–471.
19 S. Liu, M. Wei, X. Wang, C. Shi, S. Kuang and C. Ma, *Talanta*, 2020, **210**, 120628.
20 A. V. Kulbachinskiy, *Biochemistry*, 2007, **72**, 1505–1518.
21 P. Stadlbauer, P. Kuhrova, L. Vicherek, P. Banas, M. Otyepka, L. Trantirek and J. Sponer, *Nucleic Acids Res.*, 2019, **47**, 7276–7293.
22 H. Xi, M. Juhas and Y. Zhang, *Biosens. Bioelectron.*, 2020, **167**, 112494.
23 K. Sefah, D. Shangguan, X. Xiong, M. B. O'Donoghue and W. Tan, *Nat. Protoc.*, 2010, **5**, 1169–1185.
24 Y. Zhang, Y. Wu, H. Zheng, H. Xi, T. Ye, C.-Y. Chan and C. K. Kwok, *Anal. Chem.*, 2021, **93**, 5744–5753.
25 B. I. Fedeles, *Proc. Natl. Acad. Sci. U. S. A.*, 2017, **114**, 2788–2790.
26 J. E. Johnson, J. S. Smith, M. L. Kozak and F. B. Johnson, *Biochimie*, 2008, **90**, 1250–1263.
27 L. Peng, Q. Xi, X. Wang, Y. Kan, J. Jiang and R. Yu, *Anal. Lett.*, 2014, **47**, 2341–2349.
28 L. Guo, D. Nie, C. Qiu, Q. Zheng, H. Wu, P. Ye, Y. Hao, F. Fu and G. Chen, *Biosens. Bioelectron.*, 2012, **35**, 123–127.
29 X. F. Zhang, H. M. Xu, L. Han, N. B. Li and H. Q. Luo, *Anal. Sci.*, 2018, **34**, 149–153.
30 M. Caragata, A. K. Shah, B. L. Schulz, M. M. Hill and C. Punyadeera, *Anal. Biochem.*, 2016, **497**, 76–82.
31 G. ZederLutz, E. Zuber, J. Witz and M. H. V. VanRegenmortel, *Anal. Biochem.*, 1997, **246**, 123–132.
32 A. Kreig, J. Calvert, J. Sanoica, E. Cullum, R. Tipanna and S. Myong, *Nucleic Acids Res.*, 2015, **43**, 7961–7970.
33 C. J. Wienken, P. Baaske, U. Rothbauer, D. Braun and S. Duhr, *Nat. Commun.*, 2010, **1**, 100.
34 M. Jerabek-Willemsen, C. J. Wienken, D. Braun, P. Baaske and S. Duhr, *Assay Drug Dev. Technol.*, 2011, **9**, 342–353.
35 S.-J. Wu, M. Soulez, Y.-H. Yang, C.-S. Chu, S.-C. Shih, M.-J. Hebert, M.-C. Kuo and Y.-J. Hsieh, *PLoS One*, 2015, **10**, e0132583.
36 D. Ji, M. Juhas, C. M. Tsang, C. K. Kwok, Y. Li and Y. Zhang, *Briefings Bioinf.*, 2021, **22**, 1150–1160.
37 S. A. I. Seidel, P. M. Dijkman, W. A. Lea, G. van den Bogaart, M. Jerabek-Willemsen, A. Lazic, J. S. Joseph, P. Srinivasan, P. Baaske, A. Simeonov, I. Katritch, F. A. Melo, J. E. Ladbury, G. Schreiber, A. Watts, D. Braun and S. Duhr, *Methods*, 2013, **59**, 301–315.
38 J. M. Nicoludis, S. P. Barrett, J. L. Mergny and L. A. Yatsunyk, *Nucleic Acids Res.*, 2012, **40**, 5432–5447.
39 Y. Suzaki, Y. Ozawa and H. Kobori, *Peptides*, 2006, **27**, 3000–3002.
40 P. C. Dedon, J. A. Soults, C. D. Allis and M. A. Gorovsky, *Anal. Biochem.*, 1991, **197**, 83–90.